

An Iron Mesoionic Carbene Complex for Catalytic Intramolecular C–H Amination Utilizing Organic Azides

Wowa Stroek,¹ Martin Keilwerth,² Daniel M. Pividori,² Karsten Meyer² and Martin Albrecht^{1,*}

¹Department of Chemistry, Biochemistry and Pharmaceutical Sciences, University of Bern, CH-3012 Bern, Switzerland

²Department of Chemistry & Pharmacy, Inorganic Chemistry, Friedrich-Alexander-University Erlangen-Nürnberg (FAU), 91058 Erlangen, Germany

KEYWORDS: C–H amination, Nitrenes, Mesoionic carbenes, *N*-heterocycles, Iron

ABSTRACT: The synthesis of *N*-heterocycles is of paramount importance for the pharmaceutical industry. They are often synthesized through atom economically and environmentally unfriendly methods, generating significant waste. A less explored, but greener alternative, is the synthesis through the direct intramolecular C–H amination utilizing organic azides. Few examples exist using this method, but many are limited due to the required use of stoichiometric amounts of Boc₂O. Herein, we report a homoleptic *C,O*-chelating mesoionic carbene iron complex, which is the first iron-based complex that does not require the addition of any protecting groups for this transformation and that is active also in strong donor solvents such as THF or even DMSO. The achieved turnover numbers are an order of magnitude higher than any other reported catalytic system. A variety of C–H bonds were activated, including benzylic, primary, secondary and tertiary. By following the reaction over time, the presence of an initiation period was determined. Kinetic studies showed a first-order dependence on substrate concentration and half-order dependence on catalyst concentration. Intermolecular competition reactions with deuterated substrate showed no KIE, while separate reactions with deuterium-labeled substrate resulted in a KIE of 2.0. Moreover, utilizing deuterated substrate significantly decreased the initiation period of the catalysis. Preliminary mechanistic studies suggest a unique mechanism involving a dimeric iron species as the catalyst resting state.

1. Introduction

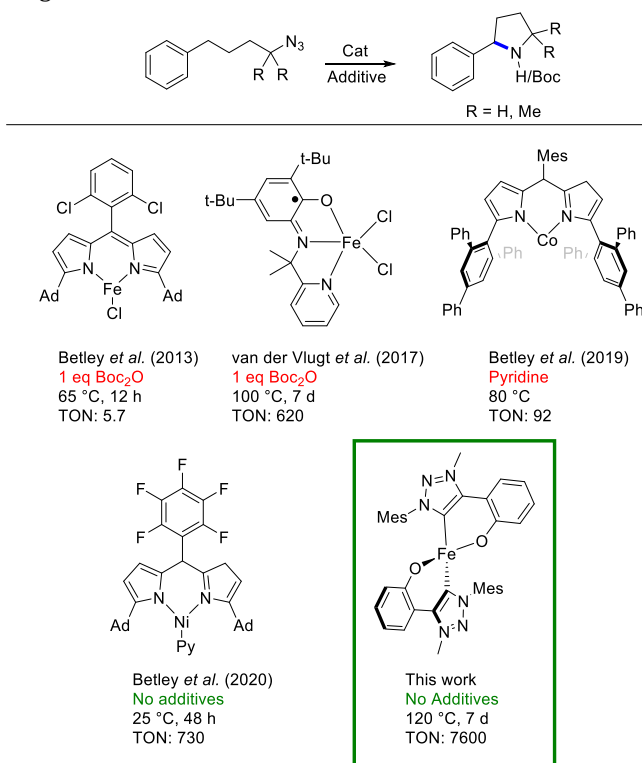
Formation of carbon-nitrogen bonds is an important step in the synthesis of pharmaceuticals, agrochemicals and natural products.¹ Of the FDA approved drugs, some 60% contain a nitrogen heterocycle, making them an important class of C–N bond containing compounds in the pharmaceutical industry.^{2,3} Among them are for example the strong opioid pain relievers oxycodone⁴ and morphine,⁵ blood thinners apixaban⁶ and rivaroxaban,⁷ paroxetine⁸ used as an antidepressant, and methylphenidate⁹ to treat ADHD. Many of them are listed in the top 200 sold drugs worldwide.¹⁰

Formation of the C–N bond makes the synthesis of this class of compounds challenging, common methods to form C–N bonds are nucleophilic substitution, cycloadditions and reductive aminations.^{11,12} These methods often require additional synthetic steps, in order to install the required functional groups. More attractive, but far less developed methods are nitrene transfer reactions, such as direct C–H amination or alkene aziridination, which are often catalyzed by transition metal complexes.^{13,14} Even though many different methods are available for the generation of the highly active nitrene, most of them suffer from a poor atom economy, as they are derived from *e.g.* hypervalent iodides,¹⁵ and therefore generate significant amounts of waste products.^{15,16} Arguably, the most atom-economic nitrene precursors are organic azides, as dinitrogen is the only waste product formed upon nitrene generation.

Pioneering work by Betley *et al.* revealed the synthesis of *N*-heterocycles by direct intramolecular C–H amination using azides in the presence of an iron-dipyrin catalyst and stoichiometric amounts of Boc₂O in order to form protected *N*-heterocycles (Scheme 1).¹⁷ While turnover numbers (TONs) were low (5.7), this work demonstrated the feasibility of using azides. Several hundreds of TONs were accomplished with van der Vlugt's iron complex bearing a redox-active NNO ligand, though stoichiometric amounts of Boc₂O were still needed to prevent catalyst inhibition by the amine product (Scheme 1).¹⁸ Direct C–H amination with azides was also demonstrated with cobalt,^{19,20} iron^{21–24} and palladium^{25,26} catalysts, but they were all limited by the use of Boc₂O. Only recently, Betley *et al.* developed a cobalt- and a nickel-dipyrin system, which operate at room temperature and do not require addition of Boc₂O or other protecting groups.^{27,28} Key was the availability of pyridine, either as an additive or as a built-in ligand, to suppress catalyst deactivation (Scheme 1). However, TONs remained moderate and all catalysts known so far of Earth-abundant iron require stoichiometric amounts of Boc₂O, which produces considerable amounts of waste and deteriorates the atom-economy of this reaction.

Based on our experience in utilizing mesoionic carbenes (MICs) in catalytic transformations,²⁹ we envisioned that their extremely electron donating nature disfavors amine coordination; therefore, circumventing product inhibition

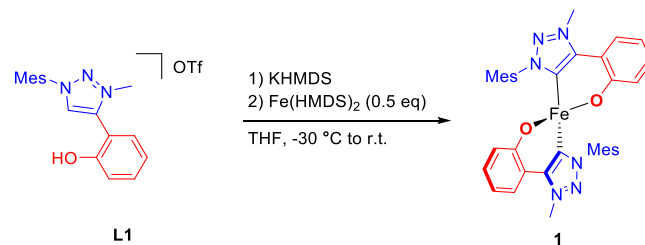
in C–H amination. Coordination of MICs to first-row transition metals has considerable catalytic potential,³⁰ though catalyst robustness is a challenge since first row transition metals, especially in high valence states, prefer ionic interactions while MIC are known to form bonds with highly covalent character. In order to tackle this mismatch, we designed a phenoxy chelating moiety, which favors ionic interactions as a means to support MIC bonding to the first-row transition metal center. Herein, we report the synthesis of a *C,O*-chelating homoleptic iron complex, which is highly active in the catalytic intramolecular C–H amination for the synthesis of *N*-heterocycles. For the first time, no addition of Boc₂O – or any other protecting group – is required with an iron catalyst, and the accomplished TONs are unprecedentedly high and surpass the state-of-the-art by one order of magnitude.



Scheme 1. Selected examples of previously reported catalysts for the intramolecular C–H amination using alkylazides, in comparison with the herein reported catalyst.^{17,18,27,28}

2. Results & Discussion

2.1 Synthesis of Iron complex 1. Iron complex **1** was synthesized from ligand **L1** by phenol deprotonation of **L1** with KHMDS (Scheme 2 and SI), followed by addition of 0.5 equivalents of Fe(HMDS)₂³¹ and stirring for 16 h. Purification by precipitation and several extractions afforded pure (by CHN combustion elemental analysis) yet highly air- and moisture-sensitive complex **1** as an orange powder. The synthetic procedure is robust and has been successfully applied to gram-scale preparations of **1**. Single-crystals suitable for X-ray diffraction analysis were obtained by laying a concentrated benzene solution of **1** with hexane.



Scheme 2. Synthesis of iron complex **1**

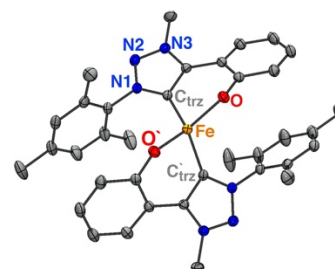


Figure 1. ORTEP representation of **1** (50% probability ellipsoids, H atoms omitted for clarity).

The molecular structure displays a highly distorted tetrahedral homoleptic iron complex ($\tau_4 = 0.79$ $\tau'_4 = 0.81$),^{32,33} in which two ligands with identical bond lengths and angles coordinate in a *C,O*-bidentate chelating fashion (Fig. 1). The high distortion is attributed to the fixed bite angle of the bidentate ligand (O–Fe–C_{trz} 90.29(4)°) and the high O...O electrostatic repulsion, which leads to a large O–Fe–O angle of 126.92(5)°. The Fe–C_{trz} bond distance is 2.0406(12) Å, which is longer than any of the previously reported Fe(II)–C_{trz} bonds, typically ranging between 1.92 and 2.02 Å.^{34–39}

Characterization of the complex by ¹H NMR spectroscopy suggests an open-shell electronic structure, due to the signals ranging from +60 and -20 ppm and absence of any multiplicity (Fig. S25). Furthermore, the complex was completely silent in ¹³C NMR spectroscopy. Magnetic susceptibility (μ_{eff}) measurements in solution by Evans Method⁴⁰ in C₆D₆ afforded a magnetic moment of 4.87 μ_B , consistent with the spin-only value (4.90 μ_B) of a quintet (S = 2) spin system,

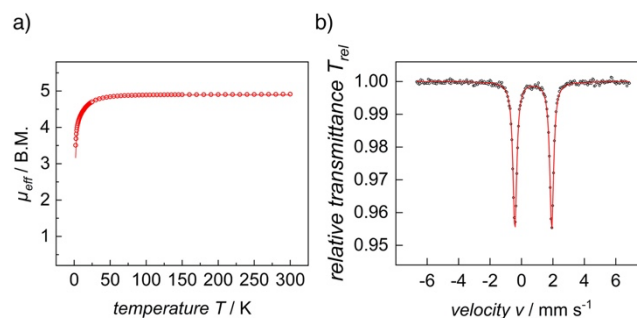


Figure 2. (a) VT-SQUID magnetization data of a solid sample of **1**, recorded with an applied DC field of 1 T, in the temperature range between 2 and 300 K. The simulation (red line) yields parameters $D = 10.03$ cm⁻¹ for the axial component of the magnetic dipole-dipole interaction, and $g_{\text{iso}} = 1.99$. For VT-VF SQUID data, see S129-S130. (b) Zero-field ⁵⁷Fe Mössbauer spectrum of a solid sample of **1**, recorded at T = 77 K. The red line represents the best fit obtained ($\delta = 0.75$ mm·s⁻¹, $\Delta E_Q = 2.34$ mm·s⁻¹, $\Gamma_{\text{fwhm}} = 0.3$ mm·s⁻¹). All simulations performed with JulX2.⁴¹

indicative of a high-spin iron(II) complex (Fig. S26-S27). SQUID measurements in the solid-state are in agreement with the magnetic data obtained from Evans Method⁴⁰ in solution and revealed a magnetic moment of 4.86 μ_B at 280 K (Fig. 2a). The equal values suggest an identical molecular structure in the solid-state and in solution. As expected for a high-spin iron(II) complex, the magnetic moment of **1** in the solid-state is temperature-independent in the 60-300 K range. Below 60 K, a sharp decrease due to zero-field splitting is noted. No spin-crossover is observed, indicating a high-spin electronic configuration of **1** over the entire 2–300 K temperature range.

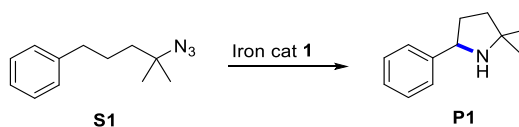
A zero-field ⁵⁷Fe Mössbauer spectrum, recorded on a powder sample of **1** at 77 K, features a single quadrupole doublet, with an isomer shift, δ , of 0.75 mm·s⁻¹ and a quadrupole splitting parameter, ΔE_Q , of 2.34 mm·s⁻¹ (Fig. 2b), indicative for the presence of a single iron species in the solid state.

2.2 Catalyst activity and optimization. To explore the reactivity of complex **1** in the intramolecular C–H amination, we initially used (4-azido-4-methylpentyl)-benzene (**S1**) as a model substrate for the formation of pyrrolidine **P1** as aminated product (Table 1). Using 1 mol% of **1** in C₆D₆ or toluene-d₈ at 100 °C resulted in a 91% yield after 24 h (entries 1-2). Formation of the pyrrolidine product was confirmed by ¹H, ¹³C NMR spectroscopy and HRMS. In addition, two minor side products were observed by ¹H NMR spectroscopy and HRMS and were identified as the linear amine formed upon reduction of the azide and the cyclic imine, respectively. The latter presumably formed by

dehydrogenation of the pyrrolidine product **P1** before product release rather than in a post-catalytic reaction, since its proportion did not increase when the reaction was kept beyond full conversion. Notably, when performing the reaction in THF-d₈, a similar yield of 88% was obtained (entry 3), contrary to previously reported iron catalysts, which are fully inhibited by THF.¹⁷ Hence, complex **1** is the first iron-based catalyst that shows catalytic activity in donor solvents, such as THF. Increasing the temperature to 120 °C in toluene-d₈ significantly increased the rate of the reaction and afforded full conversion and 92% product yield in just 6 h (entry 4). A comparable yield of 89% was obtained when using DMF-d₇ as solvent, while DMSO-d₆ decreased the rate substantially and resulted in a modest 43% yield after 6 h (entries 6-7). This drop in yield might be rationalized by the acidity of DMSO, by the presence of trace amounts of water in DMSO, or by the coordination ability of DMSO. Nonetheless, the activity in DMSO is noteworthy, since only one complex has been reportedly evaluated in DMSO to date, and that nickel-dipyrrin system displayed no catalytic activity at all in this solvent.²⁸

Remarkably, and irrespective of the solvent used, complex **1** catalyzes the intramolecular C–H amination efficiently in the absence of Boc₂O. This behavior is unique for any iron-based complex catalysing this transformation using unfunctionalized alkyl azides,²¹⁻²⁴ and indicates that the catalytically active species is not impacted by the presence of pyrrolidine product as potential ligand. Previous examples of iron complexes that do not require Boc₂O in the intramolecular C–H amination all require either aromatic or

Table 1: Optimization of the intramolecular C–H amination reaction catalyzed by **1^a.**



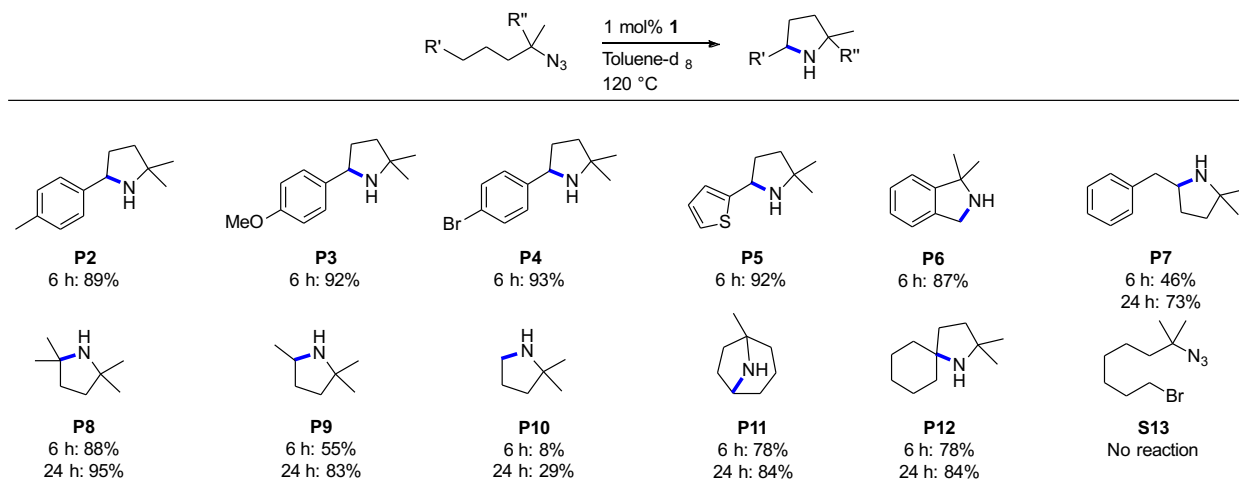
Entry	Cat loading (mol%)	Solvent	Temp. (°C)	Time	Yield (%) ^b	Conversion (%) ^b
1	1	C ₆ D ₆	100	6 h / 24 h	11 / 91	14 / 100
2	1	Toluene-d ₈	100	6 h / 24 h	12 / 91	13 / 100
3	1	THF-d ₈	100	6 h / 24 h	8 / 88	15 / 100
4	1	Toluene-d ₈	120	6 h	92	100
5 ^c	1	Toluene-d ₈	120	6 h	0	0
6	1	DMF-d ₇	120	6 h	89	100
7	1	DMSO-d ₆	120	6 h	43	46
8	0.1	Toluene-d ₈	120	48 h	78	81
9	0.01	Toluene-d ₈	120	7 d	76	81
10	0	Toluene-d ₈	120	7 d	0	0
11	1	Toluene-d ₈	25	7 d	0	0
12	1 ^d	Toluene-d ₈	120	6 h	0	0
13	1 ^e	Toluene-d ₈	120	6 h	9 / 14	10

^aCatalysis was performed on a 0.25 mmol scale in J Young NMR tubes; see SI for exact experimental details. ^bYields and conversions were determined by ¹H NMR spectroscopy using 1,3,5-trimethoxybenzene as internal standard. ^cOne equivalent of Boc₂O was added. ^dFe(OAc)₂ was used as catalyst. ^eFeCl₂ was used as catalyst.

specifically functionalized alkyl azides.^{42,43} The formation of a robust catalytic species that is insensitive to exogenous donors is also supported by the efficient catalytic transformations observed in strong donor solvents, such as THF, DMF and, to some extent, even in DMSO (*vide supra*). Surprisingly, the addition of one equivalent of Boc₂O has actually a detrimental effect and fully inhibits catalytic turnover, which was attributed to decomposition of **1** in presence of Boc₂O (entry 5). In agreement with the high robustness of the catalytically active species, lowering of the catalyst loading was possible. Using 0.1 instead of 1 mol% of **1** resulted in a 78% yield after 48 h (entry 8). Further lowering to just 0.01 mol% did not affect the yield significantly (76%, 81% conversion), though extended reaction times of 7 d were required (entry 9). This performance corresponds to 7600 TON, which is an order of magnitude higher than any other reported molecular catalyst reported to date.²⁸ No conversion was observed at room temperature, contrary to the nickel²⁸ and cobalt^{27,44} catalysts reported by Betley *et al.* Also, a blank reaction in the absence of the iron catalyst does not afford any product (entries 10-11). Similarly, simple iron salts such as Fe(OAc)₂ and FeCl₂ showed negligible catalytic activity and gave 0% and 9% yield, respectively, after 6 h, *cf.* 92% with complex **1**. These discrepancies demonstrate a clear impact of the ligand environment in **1** for imparting catalytic activity and thus support the notion of a molecularly defined active species.

The absence of α -hydrogens at the azide is crucial for high selectivity. Performing the reaction with (4-azidobutyl)benzene at 120 °C with 1 mol% **1** resulted in a mixture of multiple unidentified products (Fig. S123). While the characteristic benzylic signal for the desired pyrrolidine was observed, its quantification and hence determination of selectivity was hampered due to overlap with other resonances. We attribute the low selectivity to the high reactivity of the formed nitrene intermediate and the ensuing fast hydrogen atom abstraction (*cf.* the high activity of **1**), which leads to multiple side products when α -hydrogens and benzylic hydrogens are available. The high activity of complex **1** therefore limits the substrate scope to tertiary azides, in line with previously reported less-active systems.²⁸

2.3 Substrate scope. The scope and limitations of the **1**-catalyzed amination was explored under optimized conditions (*cf.* Table 1, entry 4) with a range of tertiary alkyl azides with different types of C–H bonds in the δ -position and with several functional groups. The tolerance of a variety of functional groups was evaluated by introducing different substituents in the para position of the model substrate. Thus, substrates with Me (**P2**), OMe (**P3**) and Br (**P4**) groups smoothly underwent C–H amination and gave comparable yields and time-conversion profiles after 6 h (Scheme 3). Accordingly, the weakly coordinating ability of aromatic ethers is not problematic, nor are aromatic bromides, despite their potential to undergo homolytic bond cleavage. Likewise, substituting the phenyl group with a weakly coordinating thiophene group (**P5**) did not result in any significant change in yield after 6 h. The catalytic system is remarkably versatile and allows for a large variety of C–H bonds to be aminated. Thus, C–H bond activation of the tolyl Ar–CH₃ group afforded the fused bicyclic isoindoline **P6** in 87% yield after 6 h (Scheme 3), indicating that primary C–H bonds are also prone to be activated. Although the aliphatic C–H bond has a higher bond dissociation energy (BDE) than benzylic C–H bonds,⁴⁵ using (5-azido-5-methylhexyl)benzene as substrate, afforded the kinetically favorable five membered heterocyclic amine **P7** in a 73% yield after 24 h. Formation of the thermodynamically more favorable six-membered ring was not observed, insinuating that the selectivity-determining step of the reaction is kinetically controlled. Furthermore, the successful transformation suggests that **1** may also catalyze the amination of unactivated strong aliphatic C–H bonds. Indeed, non-aromatic substrates with tertiary, secondary, and primary aliphatic C–H bonds in δ -position were amenable to catalytic amination and provided products **P8–P10**. Yields obtained for amines **P8–P10** are gradually declining as the BDE increases from tertiary to secondary and to primary C–H bonds in the corresponding substrates.⁴⁵ Especially the formation of amine **P10** from the activation of a primary C–H



Scheme 3. Substrate scope of the intramolecular C–H amination, blue thick bond represents the formed bond upon cyclization. Catalysis was performed on a 0.25 mmol scale in J Young NMR tubes; see SI for exact experimental details. Yields were determined by ¹H NMR spectroscopy using 1,3,5-trimethoxybenzene as internal standard.

bond proved to be challenging, in line with previous observations.^{17,28,44} Bridged bicyclic amine **P11** and bicyclic spiro amine **P12** were both obtained from their corresponding azide upon cyclization in high yields. We note that substrate **S13** featuring an alkyl bromide did not show any activity in C–H amination, presumably because of bromide abstraction by the iron catalyst as demonstrated with Betley's nickel-dipyrrin system.²⁸

2.4 Kinetic studies. Insights into the mechanism of the C–H amination of complex **1** was sought from kinetic studies. Attempts to follow the fate of **1** under catalytic conditions by ¹H NMR spectroscopy revealed no change in signals for **1** upon addition of substrate **S1** at room temperature. When heating the reaction to 120 °C, *i.e.* the temperature used for catalytic conversion, ¹H NMR spectra (at room temperature) showed a gradual decrease of the signals for **1** over time. When utilizing 1 mol% of catalyst, all signals corresponding to **1** disappeared within 2 h (Fig. S4), suggesting that the catalyst requires an activation step to form the active species. No new signals were observed, which points to an NMR-silent active species/resting state.

Reaction orders were determined by varying the starting concentration of both substrate and catalyst by using the azide **S1** under optimized conditions (Table 1, entry 4). Notably, time-dependent monitoring of the conversion reveals an induction period (Fig. 3a), in line with a catalyst activation step and an initiation phase before reaching the highest rate, consistent with the ¹H NMR spectroscopic observations (*vide supra*). Variation of the substrate concentration at constant catalyst concentration indicates that the initiation is faster at higher starting concentration of substrate **S1**, as the highest reaction rate is reached earlier (Fig. 3a). This maximum reaction rate correlates linearly with the initial substrate concentration, in excellent agreement with a first-order dependence of the reaction rate on substrate concentration for the catalytic C–H amination (Fig. 3b).⁴⁶ This dependence is in sharp contrast to most other observed rate laws reported for this reaction, in which the substrate concentration has a zero-order dependence. Only the cobalt porphyrin system by de Bruin *et al.* also has a first-order dependence on substrate.¹⁹

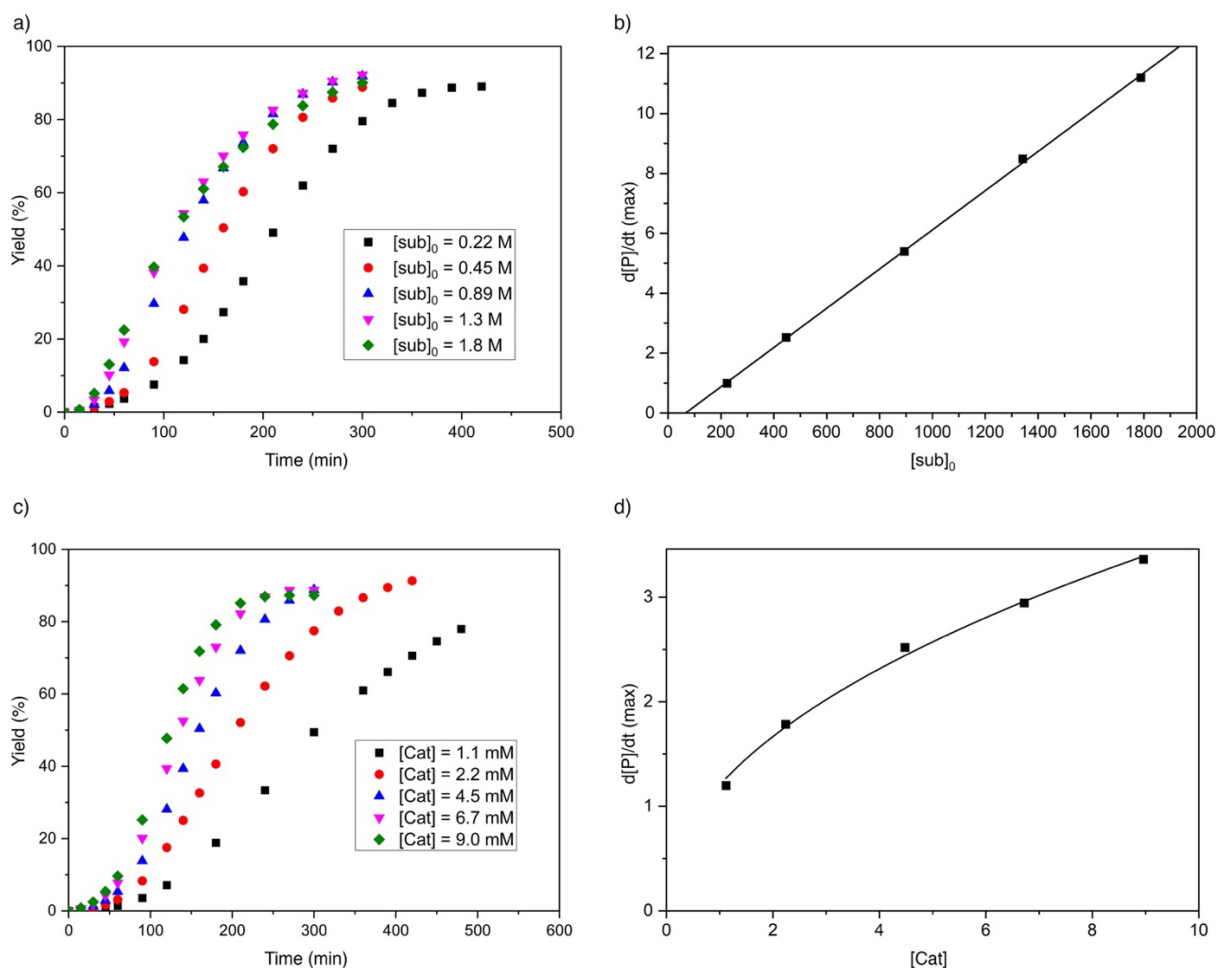


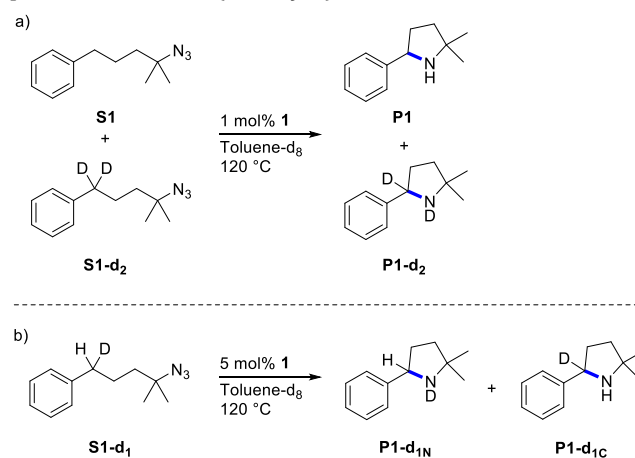
Figure 3. (a) Yield of the N-heterocycle **P1** by intramolecular C–H amination over time with varying substrate concentrations at $t = 0$, $[\text{sub}]_0 = 0.22 - 1.8 \text{ M}$, and with $[\text{cat}] = 4.5 \text{ mM}$. (b) Variation of the maximum reaction rate against substrate concentrations at $t=0$, $[\text{sub}]_0 = 0.22 - 1.8 \text{ M}$, and with $[\text{cat}] = 4.5 \text{ mM}$ together with a linear regression fit (solid line, $R^2 = 0.9996$). (c) Yield of the N-heterocycle **P1** by intramolecular C–H amination over time with varying catalyst concentrations $[\text{cat}] = 1.1 - 9.0 \text{ mM}$ and with $[\text{sub}]_0 = 0.45 \text{ M}$. (d) Variation of the maximum reaction rate against catalyst concentrations $[\text{cat}] = 1.1 - 9.0 \text{ mM}$ and with $[\text{sub}]_0 = 0.45 \text{ M}$ together with a power function fit $dP/dt = 1.17[\text{cat}]^{0.5}$ (solid line, $R^2 = 0.995$).

The rate order in catalyst was probed by varying the concentration of iron complex **1** while keeping the starting concentration of substrate **S1** unchanged. Again, the catalyst initiation period is shorter with higher catalyst concentrations (Fig. 3c). Remarkably the highest observed reaction rate is not linearly correlated with the catalyst concentration (Fig. 3d), and points to a deviation from classic first-order kinetics as observed with previously reported catalytic systems.^{17,18,25,27,28} Instead, the data provide an excellent fit with a power equation ($y = ax^b$), where b equals 0.5, commensurate with a rate law that is half-order in catalyst (Fig. 3d). This order suggests that the catalytically active species is a dimeric structure that is cleaved in the turnover-limiting step.

The kinetic isotope effect (KIE) was measured by an intermolecular competition reaction between the non-deuterated and bis-deuterated isotopomer of the substrate (**S1** vs **S1-d₂**) in the benzylic position (Scheme 4a).^{47,48} Following the reaction over time shows a preferred selectivity for **S1-d₂** at early stages of the reaction (Fig 4a,b). However, after the catalyst initiation the product distribution (**P1** vs **P1-d₂**) is close to the starting ratio of deuterated and non-deuterated substrate, indicating no KIE. It is worth noting that this is only the second catalytic system for C–H amination that does not show any KIE next to de Bruin’s cobalt porphyrin complex.¹⁹ All other systems feature a KIE between 1.9 and as high as 38.4.^{24,44}

Notably, separate intermolecular KIE experiments provided deviating results. The initiation period of the catalyst is significantly lower when using **S1-d₂** as substrate when compared to **S1** (Fig. 4c). This behavior also rationalizes the apparent inverse KIE observed at the initial stages of the competition experiment (*cf* Fig. 4b). Likewise, monitoring the reaction by ¹H NMR spectroscopy shows a faster decrease of the signals of **1** in the presence of deuterated substrate compared to the reaction with non-deuterated **S1** (Fig. S5). Moreover, comparison of the time-conversion profiles of separate catalytic runs performed exclusively with **S1-d₂** and with non-deuterated **S1**, respectively, indicates faster catalyst activation and slower catalytic conversion for the deuterium-labeled substrate **S1-d₂**. The different rates from these separate experiments yield a KIE of 2.0. However, due to the different induction periods, the KIE values

determined by intermolecular competition experiments appear more reliable (*vide infra*).



Scheme 4. (a) Intermolecular KIE competition experiment between **S1** vs **S1-d₂**. (b) Intramolecular KIE competition reactions using **S1-d₁**.

Further KIE measurements included monodeuterated substrate **S1-d₁** to discriminate intramolecular C–H vs C–D bond activation (Scheme 4b). Time-dependent monitoring of the ratio of **P1-d_{1N}**, formed via D-atom abstraction, and **P1-d_{1C}**, produced via HAA, revealed a strong preference for the formation of **P1-d_{1C}** at early stages of the reaction, *e.g.* KIE = 14.3 at 14% yield (Table S2). During the course of the reaction this selectivity erodes significantly, *e.g.* KIE = 3.9 at 34% yield, and eventually reaches a KIE of 2.2 at late stages, indicating a progressive shift to more competitive C–D bond activation. We note that conversion of **S1-d₁** does not involve any significant initiation period, similar to the conversion of **S1-d₂** and in the intermolecular KIE competition experiment. These data point to a distinct role of the C–H/D bond at catalyst activation stage. For example, agostic stabilization of the iron center by a C–H bond is expected to be stronger than with a C–D bond, therefore imparting more substantial induction times. Once the catalytically competent species is formed, however, H atom abstraction is kinetically preferred over D atom abstraction. Such a scenario is consistent with the high KIE observed at early stages in

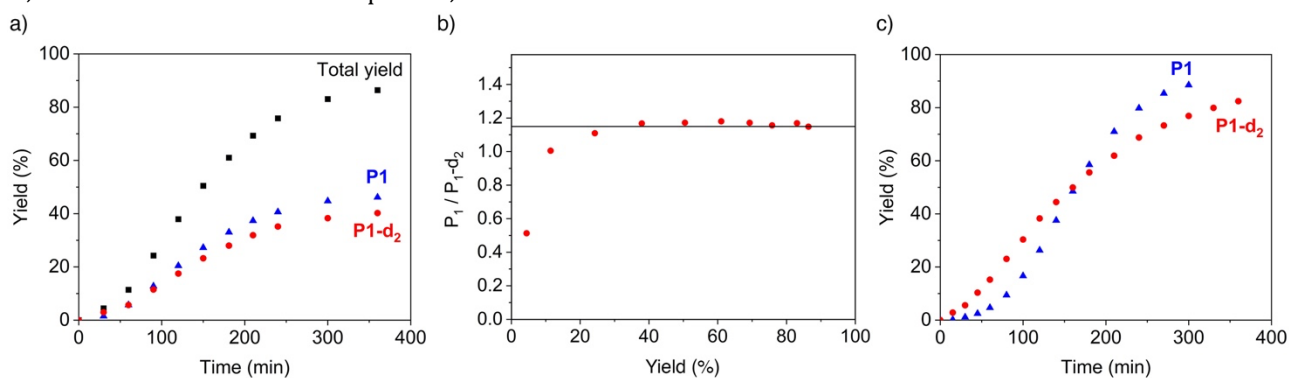


Figure 4. (a) Yield of pyrrolidine by intramolecular C–H amination over time for the intermolecular KIE competition experiment ($[S1]_0 = 0.24$ M $[S1-d_2]_0 = 0.21$ M) with $[cat] = 4.5$ mM. (b) the ratio of the deuterated and non-deuterated product **P1** with respect to the yield of the reaction, black line at 1.15 corresponds to the initial ratio of **S1** and **S1-d₂**. (c) Yield of pyrrolidine **P1** and **P1-d₂** by intramolecular C–H amination over time from isolated runs using deuterated and non-deuterated substrates **S1** and **S1-d₂** under identical conditions.

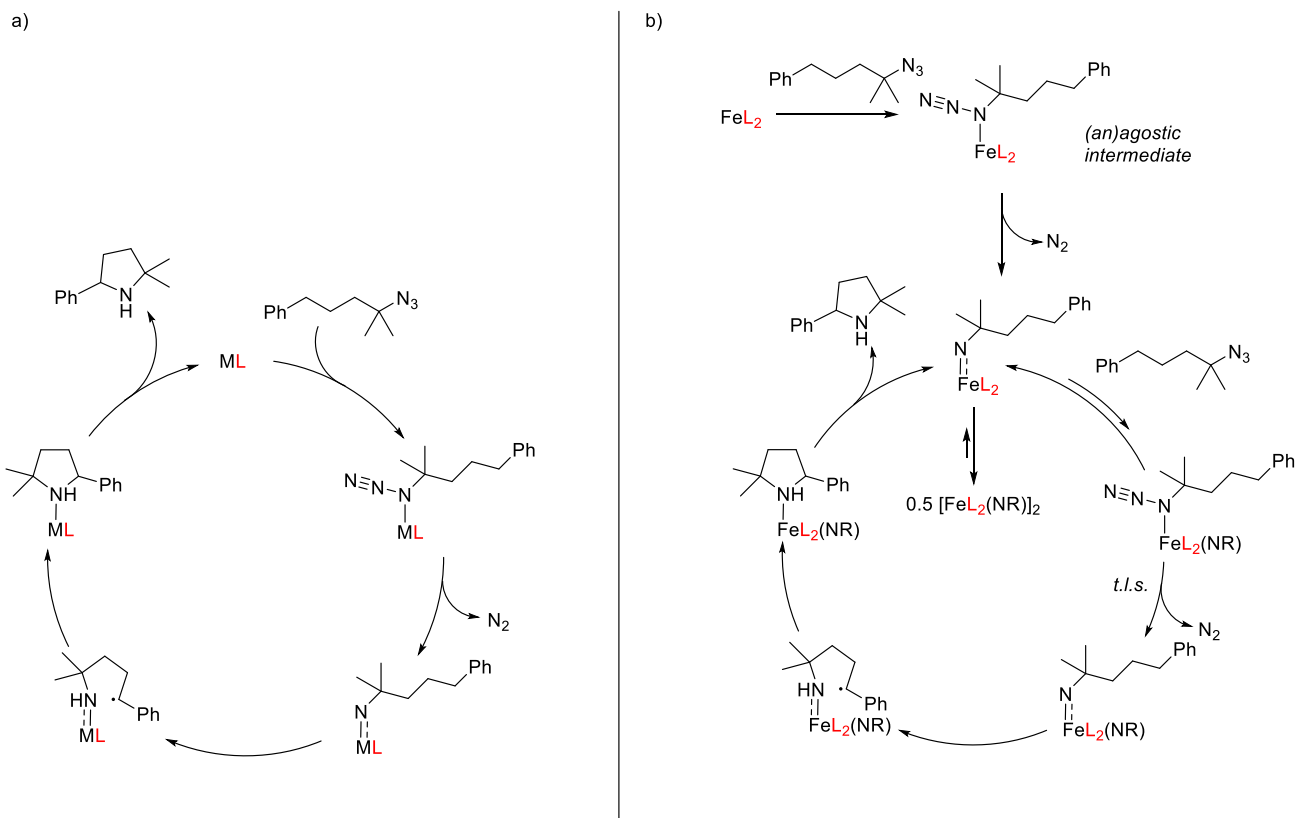
the intramolecular competition experiment, as well as with the divergences of rates and induction times observed when comparing isolated runs with **S1** and **S1-d₂**.

While formation of a non-molecular species upon catalyst activation cannot be fully excluded, the low activity of simple iron salts, the reproducible and consistent initiation period and the well-defined kinetic behavior of the catalytic system lends strong support to a catalytically active species that is molecularly defined.⁴⁹ In addition, *in situ* Evans' measurements showed a gradual change of the magnetic moment for the iron complex from 4.87 μ_B to 4.73 μ_B (Fig. S6). These data point to the formation of a new $S = 2$ complex with a slightly decreased magnetic moment, which might result from an increased diamagnetic contribution due to substrate binding or small contribution of spin states involving antiferromagnetic coupling, which is known for nitrene complexes.⁵⁰

2.5 Mechanistic considerations. All previous studies of intramolecular C–H amination utilizing azides as a nitrene precursor propose similar mechanisms (Scheme 5a).^{17–28,51} Accordingly, the first step consists of azide coordination to the metal center, followed by release of dinitrogen to obtain a metal bound nitrene. Subsequently, the nitrene undergoes a hydrogen atom abstraction (HAA) from the C–H bond, which has been identified for most reported catalysts as the turnover-limiting step based on the obtained KIE and zero-order rate dependence on substrates. An exception is the cobalt porphyrin system by de Bruin et al., in which azide coordination has been proposed as the turnover limiting step due to the observed first-order rate in substrate and

the absence of any KIE.¹⁹ The HAA step is followed by a radical recombination to form the metal-bound cyclic amine. Product release then closes the catalytic cycle. Most catalysts require Boc₂O as additive to protect the released amine and to avoid re-coordination, which is competitive to substrate coordination and typically leads to product inhibition and prevents catalyst turnover.^{17–26}

In contrast, all data on iron complex **1** indicate a distinctly different mechanism featuring a dimetallic intermediate as catalyst resting state in agreement with the prominent initiation period and the half-order rate law in catalyst concentration. Specifically, we propose formation of a dimeric iron complex, $[\text{FeL}_2(\text{NR})]_2$, upon activation of complex **1** in presence of the organic azide ($L = C, O$ -bidentate carbene ligand; Scheme 5b). Formation of this species may involve an (an)agostic interaction that is more stable with C–H bonds and therefore leads to slower catalyst activation than in the presence of weaker interactions with C–D bonds. The dimeric $[\text{FeL}_2(\text{NR})]_2$ acts as catalyst resting state and is proposed to be in equilibrium with the monomeric iron species which may be caught by an azide substrate in an unfavorable equilibrium. Subsequent irreversible loss of dinitrogen to form the iron nitrene is assumed to be the turnover limiting step. This model is consistent with the observed power one kinetics in substrate and the power half kinetics in catalyst,^{52–55} as well as the absence of any kinetic isotope effect in intramolecular competition experiments. Subsequent HAA by the nitrene and radical rebound steps may proceed in an analogous manner as deduced for other catalysts (Scheme 5a). Final amine dissociation is favored with **1**,



Scheme 5. (a) Proposed mechanism of previously reported catalytic systems for the intramolecular C–H amination using azides as a nitrene precursor; (b) diverging mechanism proposed for complex **1** (abbreviated as FeL_2 ; t.l.s. = turnover limiting step).

presumably because the stability of the dimer prevents re-coordination of the substrate. Therefore, additives like Boc₂O or pyridine^{17–26} are not required for the catalysis to proceed efficiently. The low product inhibition offers opportunities for efficient C–H amination, as demonstrated with runs producing nearly 8,000 TON.

We attribute the resistance of the catalytic cycle to donor solvents and product inhibition, in part, due to the high-spin electronic configuration of the iron complex, which decreases the interaction between the iron center and the σ -donating amine, as all d-orbitals are partially or fully occupied. In addition, unlike previously reported iron complexes that are catalytically active in this transformation, **1** bears two strongly electron donating carbene ligands; thus making the iron center highly electron rich. Moreover, the two chelating ligands shield the metal center in pseudo-tetrahedral geometry, which may induce an entatic state for high catalytic activity and simultaneously sterically shield the metal center, thus further adding to the resilience of catalytic intermediates to bind to pyrrolidine products or donor solvent molecules such as THF or DMSO.^{56,57}

3. Conclusion

We present a new open-shell homoleptic iron complex bearing two chelating phenoxy-carbene ligands as the first example of a tetrahedral complex that is active in the intramolecular C–H amination using alkylazides as nitrene precursor. The catalyst is highly robust and efficiently catalyzes the C–H amination, even at low loadings, achieving unprecedentedly high TONs of up to 7600, which is an order of magnitude higher than any other catalyst known to date. The transformation is operationally simple and highly atom-economic, since – for the first time – an iron catalyst does not require any Boc₂O when using unfunctionalized alkyl azides to prevent product inhibition typically caused by the amine. A variety of C–H bonds are activated, including tertiary, secondary, and even primary aliphatic C–H bonds, albeit the latter only in modest yields. The mode of operation of the catalyst is distinctly different when compared to other systems, and proceeds through a unique dimeric iron species. More detailed mechanistic studies to characterize relevant catalytic intermediates and to elucidate the catalyst activation process are currently ongoing in our laboratory.

ASSOCIATED CONTENT

Supporting Information. Supporting Information. Experimental details, synthetic procedures, NMR spectra, HRMS, CHN reports, SQUID data, crystallographic data, detailed catalytic procedures. This material is available free of charge via the Internet at <http://pubs.acs.org>.

AUTHOR INFORMATION

Corresponding Author

* Martin Albrecht. Martin.albrecht@unibe.ch

Notes

The authors declare no competing financial interest.

ACKNOWLEDGMENT

The authors thank Dide Verhoeven and Alex Bukvic for fruitful discussion, Lewis Maddock for technical assistance, and the X-ray crystal structure determination service unit of the Department of Chemistry, Biochemistry and Pharmaceutical Sciences of the University of Bern for crystallographic analyses. M.A. and W.S. acknowledge generous financial support from SNSF (20020_182633) and ERC (CoG 615653), and K.M. is grateful for generous funding from the Friedrich-Alexander-University Erlangen-Nürnberg (FAU).

REFERENCES

- (1) Hili, R.; Yudin, A. K. Making Carbon-Nitrogen Bonds in Biological and Chemical Synthesis. *Nat. Chem. Biol.* **2006**, *2*, 284–287.
- (2) Vitaku, E.; Smith, D. T.; Njardarson, J. T. Analysis of the Structural Diversity, Substitution Patterns, and Frequency of Nitrogen Heterocycles among U.S. FDA Approved Pharmaceuticals. *J. Med. Chem.* **2014**, *57*, 10257–10274.
- (3) Taylor, R. D.; Maccoss, M.; Lawson, A. D. G. Rings in Drugs. *J. Med. Chem.* **2014**, *57*, 5845–5859.
- (4) Moradi, M.; Esmaeili, S.; Shoar, S.; Safari, S. Use of Oxycodone in Pain Management. *Anesth Pain Med.* **2012**, *1*, 262–264.
- (5) Wang, J. K.; Nauss, L. A.; Thomas, J. E. Pain Relief by Intrathecally Applied Morphine in Man. *Surv. Anesthesiol.* **1979**, *23*, 384.
- (6) Roser-Jones, C.; Becker, R. C. Apixaban: An Emerging Oral Factor Xa Inhibitor. *J. Thromb. Thrombolysis* **2010**, *29*, 141–146.
- (7) Eriksson, B. I.; Borris, L. C.; Dahl, O. E.; Haas, S.; Huisman, M. V.; Kakkar, A. K.; Misselwitz, F.; Muehlhofer, E.; Kälebo, P. Dose-Escalation Study of Rivaroxaban (BAY 59-7939) - an Oral, Direct Factor Xa Inhibitor - for the Prevention of Venous Thromboembolism in Patients Undergoing Total Hip Replacement. *Thromb. Res.* **2007**, *120*, 685–693.
- (8) Bourin, M.; Chue, P.; Guillon, Y. Paroxetine: A Review. *CNS Drug Rev.* **2006**, *7*, 25–47.
- (9) Challman, T. D.; Lipsky, J. J. Methylphenidate: Its Pharmacology and Uses. *Mayo Clin. Proc.* **2000**, *75*, 711–721.
- (10) McGrath, N. A.; Brichacek, M.; Njardarson, J. T. A Graphical Journey of Innovative Organic Architectures That Have Improved Our Lives. *J. Chem. Educ.* **2010**, *87*, 1348–1349.
- (11) Candeias, N. R.; Branco, L. C.; Gois, P. M. P.; Afonso, C. A. M.; Trindade, A. F. More Sustainable Approaches for the Synthesis of N-Based Heterocycles. *Chem. Rev.* **2009**, *109*, 2703–2802.
- (12) Deiters, A.; Martin, S. F. Synthesis of Oxygen- and Nitrogen-Containing Heterocycles by Ring-Closing Metathesis. *Chem. Rev.* **2004**, *104*, 2199–2238.
- (13) Nakamura, I.; Yamamoto, Y. Transition-Metal-Catalyzed Reactions in Heterocyclic Synthesis. *Chem. Rev.* **2004**, *104*, 2127–2198.
- (14) Gandeepan, P.; Mu, T.; Zell, D.; Cera, G.; Warratz, S.; Ackermann, L. 3d Transition Metals for C–H Activation. *Chem. Rev.* **2019**, *119*, 2192–2452.
- (15) Park, Y.; Kim, Y.; Chang, S. Transition Metal-Catalyzed C–H Amination: Scope, Mechanism, and Applications. *Chem. Rev.* **2017**, *117*, 9247–9301.
- (16) Wang, P.; Deng, L. Recent Advances in Iron-Catalyzed C–H Bond Amination via Iron Imido Intermediate. *Chinese J. Chem.* **2018**, *36*, 1222–1240.
- (17) Hennessy, E. T.; Betley, T. A. Complex N-Heterocycle Synthesis via Iron-Catalyzed, Direct C–H Bond Amination. *Science* **2013**, *340*, 591–595.
- (18) Bagh, B.; Broere, D. L. J.; Sinha, V.; Kuijpers, P. F.; Van Leest, N. P.; De Bruin, B.; Demeshko, S.; Siegler, M. A.; Van Der Vlugt, J. I. Catalytic Synthesis of N-Heterocycles via Direct C(Sp³)-H Amination Using an Air-Stable Iron(III) Species with a Redox-Active Ligand. *J. Am. Chem. Soc.* **2017**, *139*, 5117–5124.
- (19) Kuijpers, P. F.; Tiekink, M. J.; Breukelaar, W. B.; Broere, D. L. J.; van Leest, N. P.; van der Vlugt, J. I.; Reek, J. N. H.; de Bruin, B. Cobalt-Porphyrin-Catalysed Intramolecular Ring-Closing C–H Amination of Aliphatic Azides: A Nitrene-Radical

- Approach to Saturated Heterocycles. *Chem. Eur. J.* **2017**, *23*, 7945–7952.
- (20) Goswami, M.; Geuijen, P.; Reek, J. N. H.; de Bruin, B. Application of [Co(Corrole)]– Complexes in Ring-Closing C–H Amination of Aliphatic Azides via Nitrene Radical Intermediates. *Eur. J. Inorg. Chem.* **2018**, 617–626.
- (21) Thacker, N. C.; Lin, Z.; Zhang, T.; Gilhula, J. C.; Abney, C. W.; Lin, W. Robust and Porous β -Diketiminato-Functionalized Metal-Organic Frameworks for Earth-Abundant-Metal-Catalyzed C–H Amination and Hydrogenation. *J. Am. Chem. Soc.* **2016**, *138*, 3501–3509.
- (22) Iovan, D. A.; Wilding, M. J. T.; Baek, Y.; Hennessy, E. T.; Betley, T. A. Diastereoselective C–H Bond Amination for Disubstituted Pyrrolidines. *Angew. Chem., Int. Ed.* **2017**, *56*, 15599–15602.
- (23) Du, Y. D.; Xu, Z. J.; Zhou, C. Y.; Che, C. M. An Effective [Fe III (TF 4 DMAP)Cl] Catalyst for C–H Bond Amination with Aryl and Alkyl Azides. *Org. Lett.* **2019**, *21*, 895–899.
- (24) Shing, K. P.; Liu, Y.; Cao, B.; Chang, X. Y.; You, T.; Che, C. M. N-Heterocyclic Carbene Iron(III) Porphyrin-Catalyzed Intramolecular C(Sp³)-H Amination of Alkyl Azides. *Angew. Chem., Int. Ed.* **2018**, *57*, 11947–11951.
- (25) Broere, D. L. J.; De Bruin, B.; Reek, J. N. H.; Lutz, M.; Dechert, S.; Van Der Vlugt, J. I. Intramolecular Redox-Active Ligand-to-Substrate Single-Electron Transfer: Radical Reactivity with a Palladium(II) Complex. *J. Am. Chem. Soc.* **2014**, *136*, 11574–11577.
- (26) Broere, D. L. J.; Van Leest, N. P.; De Bruin, B.; Siegler, M. A.; Van Der Vlugt, J. I. Reversible Redox Chemistry and Catalytic C(Sp³)-H Amination Reactivity of a Paramagnetic Pd Complex Bearing a Redox-Active o-Aminophenol-Derived NNO Pincer Ligand. *Inorg. Chem.* **2016**, *55*, 8603–8611.
- (27) Baek, Y.; Betley, T. A. Catalytic C–H Amination Mediated by Dipyrrin Cobalt Imidos. *J. Am. Chem. Soc.* **2019**, *141*, 7797–7806.
- (28) Dong, Y.; Clarke, R. M.; Porter, G. J.; Betley, T. A. Efficient C–H Amination Catalysis Using Nickel-Dipyrrin Complexes. *J. Am. Chem. Soc.* **2020**, *142*, 10996–11005.
- (29) Vivancos, Á.; Segarra, C.; Albrecht, M. Mesoionic and Related Less Heteroatom-Stabilized N-Heterocyclic Carbene Complexes: Synthesis, Catalysis, and Other Applications. *Chem. Rev.* **2018**, *118*, 9493–9586.
- (30) Bertini, S.; Rahaman, M.; Dutta, A.; Schollhammer, P.; Rudnev, A. V.; Gloaguen, F.; Broekmann, P.; Albrecht, M. Oxo-Functionalised Mesoionic NHC Nickel Complexes for Selective Electrocatalytic Reduction of CO₂ to Formate. *Green Chem.* **2021**, *23*, 3365–3373.
- (31) Andersen, R. A.; Faegri, K.; Green, J. C.; Haaland, A.; Lappert, M. F.; Leung, W.; Rypdal, K. Synthesis of Bis [Bis(Trimethylsilyl) Amido] Iron(II). Structure and Bonding in M[N(SiMe₃)₂]₂ (M = Mn, Fe, Co): Two-Coordinate Transition-Metal Amides. *Inorg. Chem.* **1988**, *27*, 1782–1786.
- (32) Yang, L.; Powell, D. R.; Houser, R. P. Structural Variation in Copper(I) Complexes with Pyridylmethylamide Ligands: Structural Analysis with a New Four-Coordinate Geometry Index, T₄. *Dalt. Trans.* **2007**, 955–964.
- (33) Okuniewski, A.; Rosiak, D.; Chojnacki, J.; Becker, B. Coordination Polymers and Molecular Structures among Complexes of Mercury(II) Halides with Selected 1-Benzoylthioureas. *Polyhedron* **2015**, *90*, 47–57.
- (34) Johnson, C.; Albrecht, M. Triazolylidene Iron(II) Piano-Stool Complexes: Synthesis and Catalytic Hydrosilylation of Carbonyl Compounds. *Organometallics* **2017**, *36*, 2902–2913.
- (35) Iwasaki, H.; Yamada, Y.; Ishikawa, R.; Koga, Y.; Matsubara, K. Isolation and Structures of 1,2,3-Triazole-Derived Mesoionic Biscarbenes with Bulky Aromatic Groups. *Eur. J. Org. Chem.* **2016**, 1651–1654.
- (36) Liu, Y.; Kjær, K. S.; Fredin, L. A.; Chábera, P.; Harlang, T.; Canton, S. E.; Lidin, S.; Zhang, J.; Lomoth, R.; Bergquist, K. E.; Persson, P.; Wärnmark, K.; Sundström, V. A Heteroleptic Ferrous Complex with Mesoionic Bis(1,2,3-Triazol-5-Ylidene) Ligands: Taming the MLCT Excited State of Iron(II). *Chem. Eur. J.* **2015**, *21*, 3628–3639.
- (37) Johnson, C.; Albrecht, M. Z-Selective Alkyne Semi-Hydrogenation Catalysed by Piano-Stool N-Heterocyclic Carbene Iron Complexes. *Catal. Sci. Technol.* **2018**, *8*, 2779–2783.
- (38) Liang, Q.; Hayashi, K.; Rabeda, K.; Jimenez-Santiago, J. L.; Song, D. Piano-Stool Iron Complexes as Precatalysts for Gem-Specific Dimerization of Terminal Alkynes. *Organometallics* **2020**, *39*, 2320–2326.
- (39) Nylund, P. V. S.; Nathalie, C. S.; Albrecht, M. Highly Modular Piano-Stool N - Heterocyclic Carbene Iron Complexes: Impact of Ligand Variation on Hydrosilylation Activity. *Organometallics* **2021**, *40*, 1538–1550.
- (40) Evans, D. F. The Determination of the Paramagnetic Susceptibility of Substances in Solution by Nuclear Magnetic Resonance. *J. Chem. Soc.* **1959**, 2003–2005.
- (41) E. Bill, SQUID Program JulX2, 2019.
- (42) Alt, I. T.; Guttroff, C.; Plietker, B. Iron-Catalyzed Intramolecular Aminations of C(Sp³)-H Bonds in Alkylaryl Azides. *Angew. Chem., Int. Ed.* **2017**, *56*, 10582–10586.
- (43) Liang, S.; Zhao, X.; Yang, T.; Yu, W. Iron-Phosphine Complex-Catalyzed Intramolecular C(Sp³)-H Amination of Azides. *Org. Lett.* **2020**, *22*, 1961–1965.
- (44) Baek, Y.; Hennessy, E. T.; Betley, T. A. Direct Manipulation of Metal Imido Geometry: Key Principles to Enhance C–H Amination Efficacy. *J. Am. Chem. Soc.* **2019**, *141*, 16944–16953.
- (45) Luo, Y.-R. *Comprehensive Handbook of Chemical Bond Energies*; CRC Press, Taylor & Francis Group, Boca Raton, 2007, pp. 19-48.
- (46) Notably, the graph suggests that a minimum substrate concentration is required to observe any rate, or that at very low substrate concentration, the rate is actually negative. This trend is presumably caused by the fact that the measured maximum rate is consistently underestimated here as it was determined from the slope between two data points.
- (47) Simmons, E. M.; Hartwig, J. F. On the Interpretation of Deuterium Kinetic Isotope Effects in C–H Bond Functionalizations by Transition-Metal Complexes. *Angew. Chem., Int. Ed.* **2012**, *51*, 3066–3072.
- (48) Gómez-Gallego, M.; Sierra, M. A. Kinetic Isotope Effects in the Study of Organometallic Reaction Mechanisms. *Chem. Rev.* **2011**, *111*, 4857–4963.
- (49) Akiyama, T.; Wada, Y.; Yamada, M.; Shio, Y.; Honma, T.; Shimoda, S.; Tsuruta, K.; Tamenori, Y.; Haneoka, H.; Suzuki, T.; Harada, K.; Tsurugi, H.; Mashima, K.; Hasegawa, J. Y.; Sato, Y.; Arisawa, M. Self-Assembled Multilayer Iron(0) Nanoparticle Catalyst for Ligand-Free Carbon-Carbon/Carbon-Nitrogen Bond-Forming Reactions. *Org. Lett.* **2020**, *22*, 7244–7249.
- (50) Van Leest, N. P.; De Bruin, B. Revisiting the Electronic Structure of Cobalt Porphyrin Nitrene and Carbene Radicals with NEVPT2-CASSCF Calculations: Doublet versus Quartet Ground States. *Inorg. Chem.* **2021**, *60*, 8380–8387.
- (51) Dong, Y.; Lund, C. J.; Porter, G. J.; Clarke, R. M.; Zheng, S. L.; Cundari, T. R.; Betley, T. A. Enantioselective C–H Amination Catalyzed by Nickel Iminyl Complexes Supported by Anionic Bisoxazoline (BOX) Ligands. *J. Am. Chem. Soc.* **2021**, *143*, 817–829.
- (52) Ryan, D. E.; Andrea, K. A.; Race, J. J.; Boyd, T. M.; Lloyd-Jones, G. C.; Weller, A. S. Amine-Borane Dehydropolymerization Using Rh-Based Precatalysts: Resting State, Chain Control, and Efficient Polymer Synthesis. *ACS Catal.* **2020**, *10*, 7443–7448.
- (53) Sewell, L. J.; Huertos, M. A.; Dickinson, M. E.; Weller, A. S.; Lloyd-Jones, G. C. Dehydrocoupling of Dimethylamine Borane Catalyzed by Rh(PCy₃)₂H₂Cl. *Inorg. Chem.* **2013**, *52*, 4509–4516.
- (54) Rosner, T.; Le Bars, J.; Pfaltz, A.; Blackmond, D. G. Kinetic Studies of Heck Coupling Reactions Using Palladacycle Catalysts: Experimental and Kinetic Modeling of the Role of Dimer Species. *J. Am. Chem. Soc.* **2001**, *123*, 1848–1855.
- (55) Kina, A.; Iwamura, H.; Hayashi, T. A Kinetic Study on Rh/Binap-Catalyzed 1,4-Addition of Phenylboronic Acid to Enones: Negative Nonlinear Effect Caused by Predominant Homochiral Dimer Contribution. *J. Am. Chem. Soc.* **2006**, *128*, 3904–3905.

(56) Comba, P. Coordination Compounds in the Entatic State. *Coord. Chem. Rev.* **2000**, 200–202, 217–245.

(57) Stanek, J.; Hoffmann, A.; Herres-Pawlis, S. Renaissance of the Entatic State Principle. *Coord. Chem. Rev.* **2018**, 365, 103–121.

For Table of Contents use only

